Civil Engineering and Architecture 13(6): 4220-4232, 2025
DOI: 10.13189/cea.2025.130610 http://www.hrpub.org

Multi-Objective Optimization of Alkali-Activated Concrete Using Fly Ash and GGBFS through Desirability Function Analysis

M. V. S. S. Sastri[1], K. Rajani Kumar[2,*], K. Jagannadha Rao[3], S. Vijaya Kumar[1]

[1]Department of Civil Engineering, Vasavi College of Engineering (A), Ibrahimbagh, Hyderabad-500031, Telangana, India
[2]Department of Chemistry, Vasavi College of Engineering (A), Hyderabad-500031, Telangan, India
[3]Department of Civil Engineering, Chaitanya Bharathi Institute of Technology (A), Hyderabad-500075, Telangana, India

Received May 29, 2025; Revised September 5, 2025; Accepted September 19, 2025

Cite This Paper in the Following Citation Styles

(a): *[1] M. V. S. S. Sastri, K. Rajani Kumar, K. Jagannadha Rao, S. Vijaya Kumar , "Multi-Objective Optimization of Alkali-Activated Concrete Using Fly Ash and GGBFS through Desirability Function Analysis," Civil Engineering and Architecture, Vol. 13, No. 6, pp. 4220 - 4232, 2025. DOI: 10.13189/cea.2025.130610.*

(b): *M. V. S. S. Sastri, K. Rajani Kumar, K. Jagannadha Rao, S. Vijaya Kumar (2025). Multi-Objective Optimization of Alkali-Activated Concrete Using Fly Ash and GGBFS through Desirability Function Analysis. Civil Engineering and Architecture, 13(6), 4220 - 4232. DOI: 10.13189/cea.2025.130610.*

Abstract This study presents the development and multi-objective optimization of alkali-activated concrete (AAC) using fly ash (FA) and ground granulated blast furnace slag (GGBFS) under ambient curing conditions (30–35 ℃, 60–70% RH). Sodium hydroxide (NaOH) with varying molarities (8M, 12M, 16M) was used along with sodium silicate to activate the FA/GGBFS blends (100:0, 75:25, 50:50, and 25:75%). The mechanical properties, such as compressive strength, split tensile strength, and flexural strength, were evaluated after 28 d of curing. The results showed that increasing the NaOH molarity significantly enhanced the mechanical performance, with the 50% FA–50% GGBFS mix at 16M yielding the highest compressive strength (71.4 MPa), split tensile strength (3.84 MPa), and flexural strength (12.3 MPa). However, increased molarity reduces the workability owing to shorter setting times and higher viscosity. To optimize the performance holistically, Desirability Function Analysis (DFA) was used to simultaneously evaluate six parameters: compressive strength, split tensile strength, flexural strength, cylindrical compressive strength, cost, and CO_2 emissions. Cost analysis focused on activators, whereas CO_2 emissions were estimated using literature-based factors (1.5 kg CO_2/kg NaOH and 0.07 kg/CO_2 GGBFS). Equal weighting was applied to all the six variables. The highest composite desirability (0.893) was achieved by the 8M NaOH, 50% FA–50% GGBFS mix, which offered strong mechanical properties (58.3 MPa compressive strength), low cost (US \$84.86/m³), and moderate CO_2 emissions (49.71 kg/m³), making it the most sustainable and structurally efficient blend. Meanwhile, the 12M–50% FA–GGBFS mix showed the highest mechanical strength and ranked second overall, balancing strength and sustainability, and was especially suitable for structural applications. This study demonstrates that AAC mixes can be tailored to meet both economic and environmental goals without compromising performance. It also confirms that ambient curing with balanced FA/GGBFS ratios enables practical AAC production for real-world applications.

Keywords Alkali Activated Concrete (AAC), Ground Granulated Blast Furnace Slag (GGBFS), Fly ash, Molarity, Solid Waste Management

1. Introduction

Concrete is the most widely used construction material due to its strength, durability, and cost-effectiveness. However, the production of Portland cement, the primary

binder in concrete requires significant natural resources and emits large amounts of CO_2, contributing to global warming [1]. To mitigate these environmental concerns, researchers are actively exploring sustainable alternatives using industrial by-products and waste materials that reduce carbon emissions and resource consumption [2].

Ground Granulated Blast Furnace Slag (GGBFS), a by-product of steel manufacturing, and fly ash (FA), generated by coal-based thermal power plants, are promising supplementary cementitious materials [3]. These materials are rich in silica and alumina, making them suitable for alkali activation to form alternative binders. Alkali-activated binders, often referred to as "inorganic polymers" or "geopolymers," are known for their high strength, durability, and low environmental impact.

Alkali-activated concrete (AAC) is produced by combining such binders with alkaline activators, typically sodium hydroxide (NaOH) and sodium silicate (Na_2SiO_3), which promote polymerization and network formation [4-6]. The resulting concrete can serve as a sustainable substitute for Portland cement concrete, especially when designed for ambient curing conditions [7]. This study explores the mechanical performance and optimization of AAC using FA and GGBFS, focusing on strength development, cost efficiency, and mix proportioning through statistical tools.

Juenger et al. [2] provided a comprehensive overview of alternative binders to Portland cement, detailing their compositions, reaction mechanisms, advantages, and limitations. Sithole and Mashifana [8] investigated the optimal alkaline activator conditions for GGBFS-based bricks, concluding that 15M NaOH, 20% liquid-to-solid ratio, and 80 ℃ curing for five days yielded the highest compressive strength.

Several studies have reported that replacing fly ash with GGBFS improves workability, setting time, and mechanical properties [9]. Jeong et al. [10] emphasized the influence of slag characteristics, particularly calcium sulfate content, fineness, and alkalinity, on the strength development in CaO-activated systems. Pavithra et al. [11] evaluated the effects of NaOH molarity (10M–18M) and Na_2SiO_3/NaOH ratios (1.0–1.5) on fly ash-based alkali-activated mortars. SEM analyses confirmed enhanced reactivity and strength with increasing molarity and silicate content. Puligilla and Mondal [12] observed accelerated setting and improved microstructure with the addition of GGBFS to fly ash-based geopolymers.

Recent studies have confirmed the effectiveness of ambient-cured alkali-activated concrete (AAC). Pradhan et al. [13] and Osman et al. [14] demonstrated that ambient-cured AAC with optimized FA and GGBFS ratios could achieve comparable strength and durability to heat-cured systems. Their findings support sustainable in-situ applications without the need for thermal curing.

In terms of ternary and hybrid systems, Maheswaran et al. [15] explored the performance of geopolymer concretes incorporating FA, GGBFS, and nano-silica. Their results showed that increased NaOH molarity and addition of nano-silica significantly enhanced sulfate resistance, reduced sorptivity, and improved matrix compactness. Similarly, nano-supplementation has attracted interest in AAC research. Samuvel et al. [16] reported that nano-GGBFS enhanced the compressive strength and refined the microstructure, while Tran et al. [17] demonstrated that graphene nanoplatelets improved the high-temperature stability and overall strength of ambient-cured one-part AAC. Arun et al. [18] examined self-compacting geopolymer concrete with GGBFS and metakaolin by applying machine learning (Random Forest, Gradient Boost, XGBoost) to predict the compressive strength. The Gradient Boost model yielded the highest accuracy (R^2= 0.929), highlighting the value of predictive tools for sustainable mix design. Kumar et al. [4] observed enhanced morphology, increased amorphous gel content, and improved mechanical strength with up to 50% GGBFS replacement. However, fly ash-based AAC often exhibits delayed setting under ambient curing, which can be overcome by incorporating calcium-rich materials, such as GGBFS, steel slag, or OPC [19, 20]. Cost-performance optimization is another crucial area of focus. Paruthi et al. [21] analyzed the economic and mechanical performance of GGBS-based geopolymer concrete with silica fume, identifying a 10% silica fume dosage as optimal. Additionally, Ament et al. [22] employed Bayesian optimization techniques to balance the strength and environmental impact of concrete, showing the promise of computational tools for sustainable concrete mix design.

Although previous studies have demonstrated the strength benefits of alkali-activated concrete (AAC), they often rely on elevated-temperature curing, which limits their field applicability. Additionally, most focus solely on optimizing strength, overlooking cost-effectiveness, and environmental impact, which are two critical factors for sustainable construction. Although some recent works have attempted multi-objective optimization, they frequently neglect key real-world considerations such as CO_2 emissions and feasibility under ambient conditions. This study addresses these gaps by applying Desirability Function Analysis (DFA) to optimize the AAC mix design, while simultaneously considering the following:

- Ambient curing (30–35°C) for practical field-scale implementation.
- Mechanical performance (compressive, split tensile, and flexural strengths)
- Cost efficiency and sustainability, including estimated CO_2 emissions from NaOH and GGBFS.

By varying FA, GGBFS ratios, and NaOH molarities under ambient curing conditions [23], this study offers a comprehensive optimization framework that balances structural performance with environmental and economic considerations, bridging the gap between laboratory studies and real-world applications.

1.1. Objectives

- To investigate the fresh and hardened properties of alkali-activated concrete (AAC) incorporating fly ash (FA) and ground granulated blast furnace slag (GGBFS) under ambient curing conditions.
- To evaluate the influence of NaOH molarity and FA/GGBFS ratios on workability, compressive strength, split tensile strength, and flexural strength of AAC.
- To perform a multi-objective optimization of AAC mix design using Desirability Function Analysis (DFA), considering performance parameters: mechanical strengths, material cost and CO_2 emissions.
- To identify mix proportions that achieve an optimal balance between structural performance, economic feasibility and environmental sustainability for practical AAC applications.

1.2. Scope of the Present Work

- Molarity of NaOH used in this investigation is 8M, 12M and 16M.
- Percentages of FA/GGBFS used were (100%/0%) to (25%/75%) with increments of 25% in GGBFS.
- Evaluation of the mechanical characteristics of alkali-activated concrete incorporating Fly ash and GGBFS at room temperature.
- To carry out statistical analysis using the desirability function.

2. Materials Used

Locally available fresh river sand passing through 4.75mm IS sieve, free of organic matter was employed as fine aggregate. The sand's specific gravity was determined to be 2.52, which confirms it to be in Zone-I. As coarse aggregates, 20mm nominal size crushed granite stone aggregate was used throughout the project. The coarse aggregate was found to have a specific gravity of 2.87. Fly ash from the nearby RMC ready-mix facility was used in the investigation. The silica content of the fly ash was estimated to be about 75%. The experiment employed fly ash that had passed through a sieve with a mesh size of 90 microns. The specific gravity of fly ash is 2.38.

Ground Granulated Blast Furnace Slag (GGBFS), sourced from Tata steel, shows significant chemical and physical properties that render it an effective supplementary cementitious material. Chemically, GGBFS consists of 40.3% CaO, 43.4% SiO_2, and 12.5% Al_2O_3, with smaller amounts of Na_2O (0.9%), K_2O (0.6%), and MgO (1.5%) and a Loss on Ignition (LOI) of 2.1%. Physically, GGBFS has a specific gravity of 2.92 and exhibits a high fineness of 4000 cm²/g, which is indicative of a fine particle size distribution. Furthermore, its glass content was notably high (85%), which enhanced its reactivity in cementitious systems.

Fresh drinking water was utilized for mixing the concrete. The workability of AAC was improved by adding sulphonated naphthalene polymers at 1.5% of the mass of fly ash and GGBFS.

The sodium hydroxide utilized in this research was in flake form with a purity level of 98%. Minor impurities were below 2%, as per supplier specifications. It has a specific gravity of 1.52 and a molecular weight of 39.997 g/mol. The sodium silicate solution (Na_2SiO_3) used is sourced locally, with its composition being Na_2O at 12.65%, SiO_2 at 29.93%, and H_2O at 56.42% by mass. This substance is in liquid form and has a melting point of 318 ℃. The study aimed to assess the mechanical characteristics of AAC when fly ash is combined with GGBFS, in comparison to an AAC mix made entirely of fly ash. Figure 1 shows the photographs of the materials used in Alkali Activated Concrete preparation.

a. Sodium hydroxide flakes b.Na_2SiO_3 solution

c.GGBFS d.Coarse Aggregates

e.Fine Aggregates f.Fly ash

Figure 1. Photograph of raw materials used (a. Sodium hydroxide flakes, b. Na_2SiO_3 solution, c. GGBFS, d. Coarse aggregates, e. Fine Aggregates, f. Fly Ash)

Multiple trial mixes were executed following the mix design guidelines suggested by Hardjito and Rangan [23]. Finally, a standard design mix was adopted (Table 1).

Table 1. Mix Design Parameters and Experimental Variables for Alkali-Activated Concrete (AAC) Incorporating Fly Ash and GGBFS

Parameter	Value/Condition
Objective	Assess mechanical characteristics of AAC with FA + GGBFS vs. FA alone
Research Variables	Fly ash/GGBFS ratio
Aggregate Ratio	Fine and coarse aggregates maintained constant
Water-to-Binder Ratio	0.45
Mix Proportion (Cement: Fine: Coarse)	1 : 1.31 : 2.18
Activator-to-Binder Ratio	0.5
Na_2SiO_3 / NaOH Ratio	2.5
NaOH Concentrations	8M, 12M, 16M

2.1. Preparation of Alkaline Liquids

To make a solution, sodium hydroxide (NaOH) flakes were dissolved in water. The concentration of NaOH solids in the solution, denoted in molarity M, affected the mass of NaOH solids in the solution. A NaOH solution with a concentration of 8 M, for example, has 8 x 40 = 320 grams of NaOH solid (flakes or pellets) per litre of solution, where 40 is the molecular weight of NaOH. Similarly, with a 16M concentration, the mass of NaOH solids per kilogram of solution was determined to be 640 grams (Table 2). It's worth noting that the amount of NaOH solids was just a fraction of the mass of the NaOH solution, with water being the major component.

Table 2. Preparation of NaOH Solution for different molarities

Molarity of NaOH, Weight of NaOH (in grams)	Pellets dissolved in 1 litre of distilled water
16 Molarity	640 grams
12 Molarity	480 grams
8 Molarity	320 grams

To achieve the desired concentration, NaOH pellets were dissolved in water for one day in advance. Prior to the incorporation of fine materials, an alkaline activator was formulated by combining NaOH and Na_2SiO_3 in a 1:2.5 ratio. Ground granulated blast furnace slag (GGBFS), fly ash, and aggregates were dry mixed for three minutes, after which the activator solution was added, followed by mixing for an additional five minutes to produce fresh AAC. To enhance workability and flow, 1.5% sulphonated naphthalene polymers were added and mixed for another five minutes.

3. Mix Design Procedure

Taking into account the water absorption of the aggregates, the combined mass of the alkali-activated binders (fly ash and GGBFS) and alkaline liquid was 720 kg/m^3 (2400 – 1680). With an alkaline liquid-to-binder ratio of 0.5, the binder mass was calculated to be 480 kg/m^3, and the alkaline liquid mass was 240 kg/m^3. The sodium silicate (Na_2SiO_3) to sodium hydroxide (NaOH) mass ratio is 2.5, resulting in 69 kg/m^3 of NaOH solution and 171 kg/m^3 of Na_2SiO_3 solution. An 8 Molar NaOH solution was prepared with 40% NaOH solids and 60% water by mass. The water-to-binder mass ratio was calculated for each trial mixture. An additional 55 litres of water is estimated on a trial basis to achieve sufficient workability.

The proportions of the AAC mixture are detailed as follows: The sample mix FA50-GGBFS50 comprised a total binder mass of 480 kg/m^3, using 50% fly ash (Class F) and 50% GGBFS. Natural coarse aggregates are included in two sizes: 630 kg/m^3 of 20 mm and 420 kg/m^3 of 10 mm. Fine aggregate passing through a 4.75 mm IS sieve was used at 630 kg/m^3. The water-to-binder ratio was supplemented with an additional 55 kg/m^3 water. The alkaline solution-to-binder mass ratio was 0.5%, which ensured sufficient activation of the binder. A superplasticizer dosage of 1.5% of the binder mass was added to improve the workability and flow characteristics of fresh concrete and the cost estimation for the quantities is shown in Table 3.

3.1. Curing of Test Specimens

The minimum curing temperature required for the effective development of alkali-activated concrete (AAC) is approximately 30 ℃, which can be naturally achieved under ambient tropical conditions. In this study, all specimens were cured in air under shaded ambient conditions for 28 days, where recorded temperatures ranged between 30 ℃ and 35 ℃, with relative humidity maintained between 60-70%. Preliminary trials indicated that AAC mixes with 100% fly ash exhibited delayed setting under ambient conditions, which was mitigated by incorporating GGBFS. After demoulding, specimens were stored without external heating. Compressive strength, split tensile strength, and flexural strength were determined after 28 days of ambient curing. For each mix, three specimens were tested per strength property, and mean values were reported. To represent data variability, standard deviations were calculated and displayed as error bars in Figures 2 to 4.

Table 3. Material Quantities and Costs for Sodium Silicate and Sodium Hydroxide at Different NaOH Concentrations (8M, 12M, 16M)

Molar weight	8M	12M	16M
Solution of Sodium silicate (kg/m^3)	171		
Pellets of Sodium Hydroxide (kg/m^3)	21.94	32.91	43.89
Cost	8M Cost in USD	12M Cost in USD	16M Cost in USD
Solution Sodium silicate (kg/m^3)	67.16	67.16	67.16
Pellets Sodium Hydroxide (kg/m^3)	17.73	26.59	35.46
Total Cost in USD.	84.89	93.76	102.62

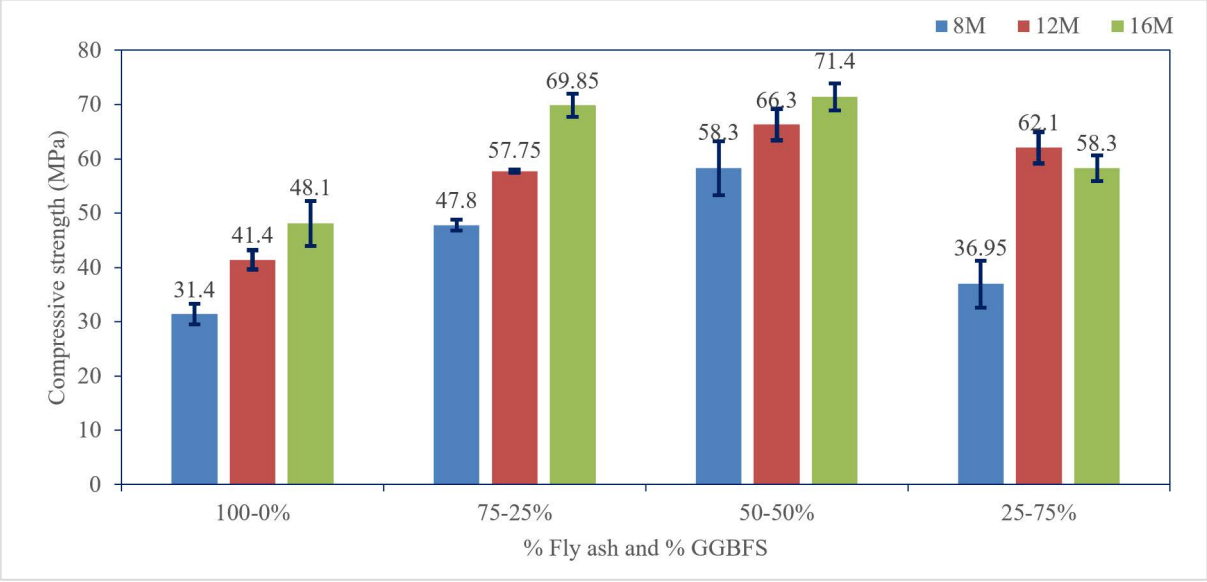

Figure 2. Variation of 28-day Compressive Strength of AAC (with Fly ash and GGBFS) with different molarities of NaOH

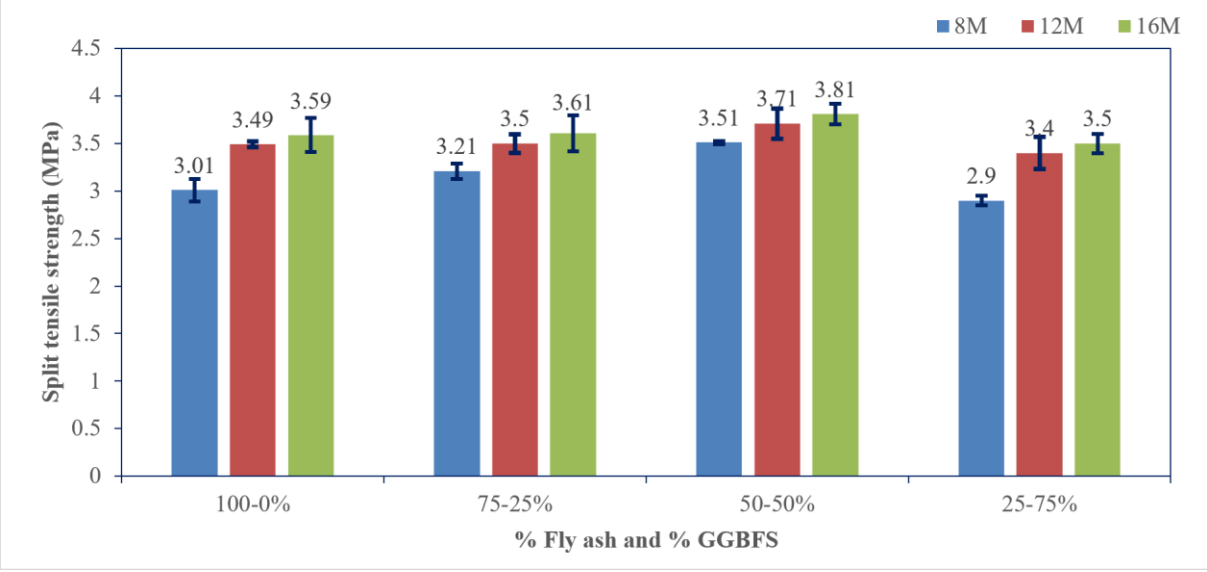

Figure 3. Variation of 28-day Split Tensile Strength of AAC (with Fly ash and GGBFS) with different molarities of NaOH

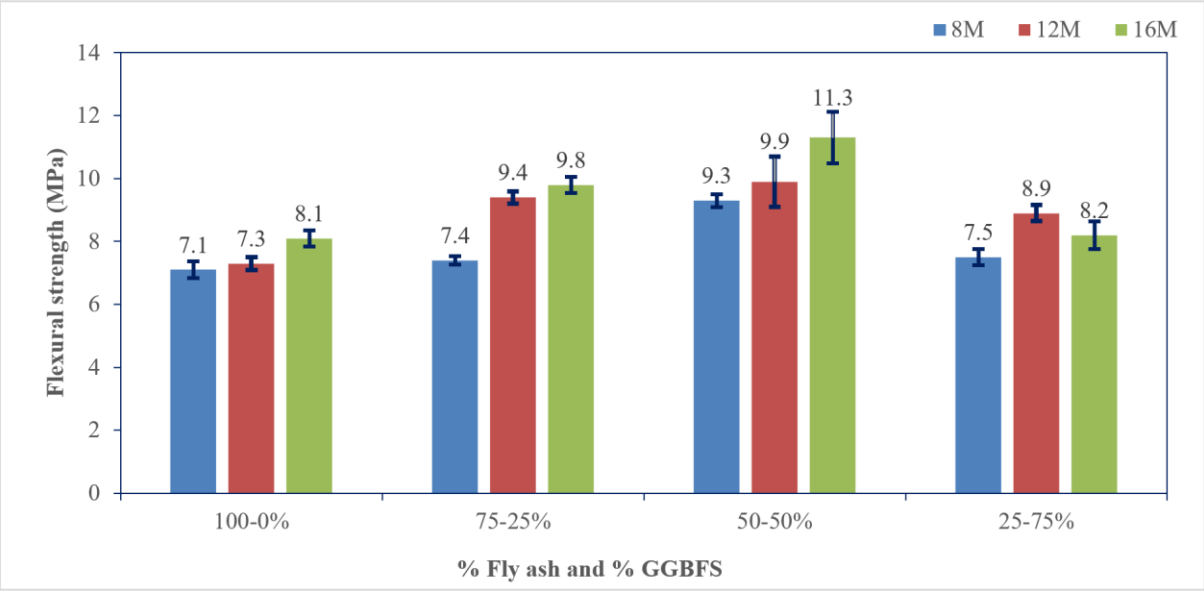

Figure 4. Variation of 28-day Flexural Strength of AAC (with Fly ash and GGBFS) with different molarities of NaOH

4. Experimental Work

Conventional AAC systems often require elevated-temperature curing; however, in this study, curing was carried out under ambient conditions (30–35 ℃) to assess the feasibility of field-scale applications. The experimentation was designed to determine the optimum molarity, low cost and combination of mineral admixtures while curing the AAC at ambient temperature, i.e. at room temperature. In this project, the samples were exposed to direct sunlight, and no additional heating was done. The highest recorded temperature during work is 35 ℃. It also investigates how much the slag in the alkali-activated fly ash/slag combination enhances the mechanical characteristics of the mixture during curing at ambient temperature. The compressive strength of cubes was determined using three numbers of 150mm size cubes after 28 days of curing. The split tensile strength was conducted on 150 mm diameter and 300mm height cylinders and the flexural strength test was done on 100mm square cross-section and 500mm long prisms after a 28-day ambience curing time. The compressive strength of AAC was found on 150mm diameter and 300mm height cylinders. The samples were exposed to daylight and cured at a 30–40 ℃ temperature. All the mechanical properties of AAC samples were tested according to standard procedures [24]. For each mix and test, three specimens were evaluated. Results are presented as mean ± standard deviation. Error bars represent standard deviation.

5. Results and Discussion

The AAC with fly ash and GGBFS was tested for cube and cylinder compressive and split tensile strength and prism flexural strength.

5.1. Discussion on Effect of Workability

It is evident from Figure 5 and Table 4 that adding GGBFS to the binder impacted the slump and compaction factor of AAC. The control AAC mixtures with 100% fly ash, for all molarity ratios, showed the highest slump and compaction factor. As the amount of slag in the combination increased, the slump and compaction factor values declined. However, the impact was more pronounced at higher slag content and molarity levels. To examine the effects of slag and molarity on workability, the slump values of group 8M mixes, 12 and 16M AAC mixes were compared. For fly ash mixes, the slump values of 8M molar are 17 and 50% higher than those of 12M and 16M mixes, respectively. The pattern is the same for other blends of fly ash and GGBFS. For a combination of FA/GGBFS at a 50% ratio, the percentage reduction in slump values is 46% for 8 to 12M and 58% for 8 to 16M, indicating that the workability of AAC decreases with an increase in the percentage of GGBFS. The workability of AAC is reduced with higher concentrations of sodium hydroxide due to higher OH concentrations. A higher percentage of fly ash replacement with GGBS also causes a decrement in flow due to the irregular shape of the particles of GGBFS. This is in agreement with the findings of other researchers [25].

5.2. Effect of GGBFS + Fly Ash on Compressive Strength

The 28-day compressive strength of all AAC mixes was higher than the target strength of 30 MPa. As shown in Figure 2, the compressive strength increased with both the NaOH molarity and incorporation of GGBFS. The control mix (100% FA, 8M NaOH) recorded 31.4 MPa, while the 50% FA–50% GGBFS mix showed significantly enhanced

strengths of 58.3 MPa (8M), 66.3 MPa (12M), and 71.4 MPa (16M). This corresponds to a 127% strength gain compared with that of the control at 16M. The enhancement in strength is attributed to the increased calcium content from GGBFS and the higher alkali activation at higher molarity levels. For the 50% GGBFS replacement level, the strength improvements over the corresponding 100% FA mixes were 86% (8M), 61% (12M), and 48% (16M). Among all the combinations, the 50:50 FA/GGBFS mix consistently exhibited the highest strength, making it the most economical and structurally optimal blend.

5.3. Effect of Fly Ash +GGBFS on Split Tensile Strength

Figure 3 presents the 28-day split tensile strength results of AAC mixes with varying FA/GGBFS ratios and NaOH molarities. The control mix (100% FA, 8M NaOH) achieved a split tensile strength of 3.01 MPa, while the 50% FA–50% GGBFS mix recorded 3.51 MPa (8M), 3.71 MPa (12M), and 3.81 MPa (16M) representing a 26.6% increase at 16M over the control. The highest strength was consistently observed with 50% GGBFS replacement, which was attributed to the improved microstructure and enhanced bonding between the paste and the aggregate owing to the additional calcium content. At the 25% and 50% GGBFS replacement levels, the strength increased by approximately 7% and 17%, respectively, compared to that of the control. However, at 75% GGBFS, a decline in strength was observed across all molarities, likely owing to poor workability, leading to inadequate compaction. Although the split tensile strengths were lower than the cube compressive strengths, as expected, mixes with up to 50% GGBFS replacement achieved values comparable to those of conventional OPC concrete, supporting the findings of previous studies [26, 27]. Overall, combining FA and GGBFS in balanced proportions enhances the tensile performance of AAC under ambient curing conditions.

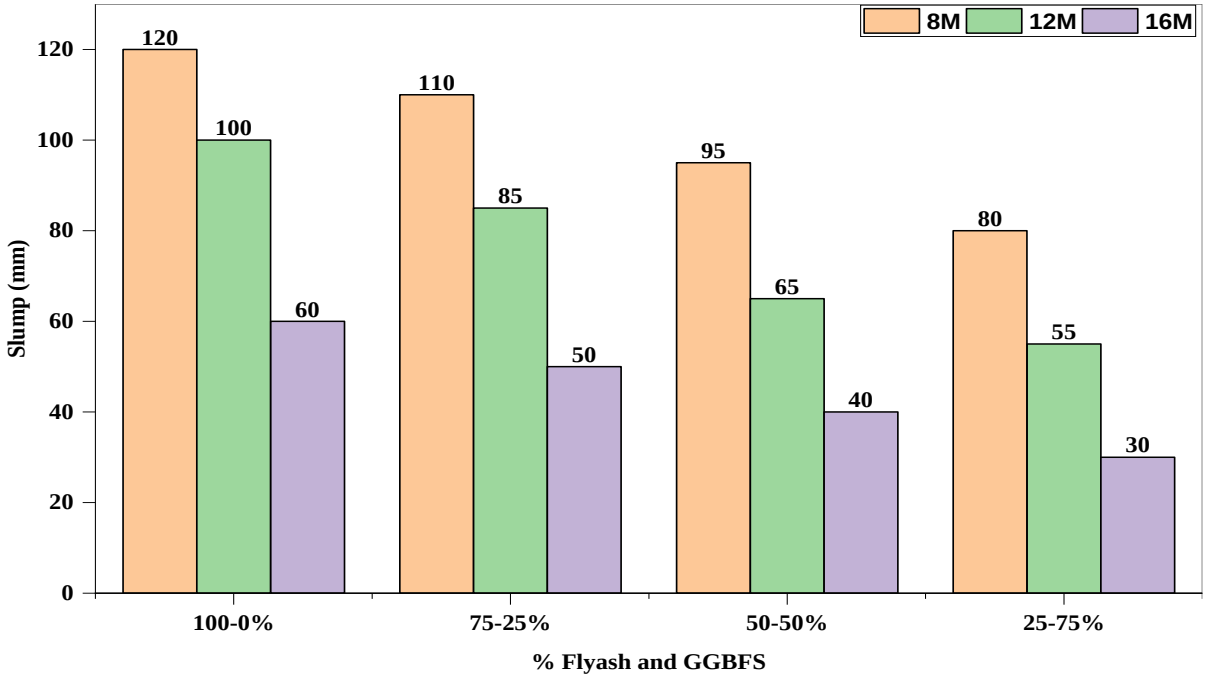

Figure 5. The variation of Slump of fresh AAC (with Fly ash and GGBFS) different molarities of NaOH

Table 4. Workability of alkali activated concrete using Fly ash and GGBFS

FA-GGBFS% →	100-0%		75-25%		50-50%		25-75%	
Molarity ↓	Slump	CF	Slump	CF	Slump	CF	Slump	CF
8M	120	0.86	110	0.83	95	0.82	80	0.84
12M	100	0.85	85	0.81	65	0.81	55	0.82
16M	60	0.83	50	0.81	40	0.79	30	0.75

5.4. Effect of GGBFS + Fly Ash on Flexural Strength

As shown in Figure 4, substituting 25% GGBFS in the concrete for the current study's 8M AAC resulted in an increase in flexural strength of 4, 31, and 6%, respectively, compared to the control concrete. As GGBFS content increased, the 28-day flexural strength rose to its maximum value at 50% substitution of Fly ash with GGBFS for all molarities before falling. A similar pattern was seen in flexural strength as well. Flexure strength for alkaline activated concrete with 50% Fly ash+ GGBFS is 11.3 MPa for 16-M concrete and subsequently declines to 7.1 N/mm^2 for 8M concrete. However, the strength of control concrete is declining by 19%, 10%, and 27% for concrete with a GGBFS of 75% compared to concrete with a GGBFS of 50%. The relatively lower flexural strength for the 16M mix, despite high compressive strength, may be due to reduced workability leading to inadequate compaction during casting, particularly affecting flexural behaviour.

The strength improvements with increased GGBFS are consistent with Samuvel et al. [16], who reported enhanced reactivity. However, our ambient curing approach differs from heat-cured studies like Pradhan et al. [13], confirming practical applicability. The decline in workability at higher molarity agrees with Sun et al. [25].

5.5. Discussion on Standard Deviation and Variability in Mechanical Properties Results

The inclusion of the standard deviation (SD) in Figures 2–4 gives valuable insights into the reliability and repeatability of the mechanical strength results for AAC mixes. Across compressive, split tensile and flexural strength tests, the SD values were consistently within ±5–8% of the mean, indicating controlled variability and stable production quality under ambient curing conditions. This narrow spread confirms that the observed performance trends, particularly the superior mechanical strengths of the 50% FA-50% GGBFS mixes are statistically robust compared to the result of outlier data points [28].

For compressive strength, mixes with higher GGBFS content exhibited slightly lower SD values compared to 100% FA mixes, likely due to the stabilizing effect of calcium-rich slag on the reaction kinetics and microstructural development. In the split tensile and flexural strength tests, the SD values tended to increase marginally at higher NaOH molarities (16M) which can be attributed to the reduced workability and potential inconsistencies in compaction during specimen preparation [29].

From a practical standpoint, the low variability strengthens the confidence in scaling up these AAC mixes for field applications because consistent performance is critical for structural reliability. From a sustainability perspective, the low SD in high-performing mixes, such as the 8M–50% FA-GGBFS and 12M–50% FA-GGBFS blends, suggests that eco-efficient mixes can be produced with repeatable quality, supporting broader adoption [30].

5.6. Simultaneous Optimization of Strength and Cost of AAC

Evaluating the sustainability of alkali-activated concrete (AAC) requires the simultaneous consideration of multiple factors, particularly the mechanical performance and economic feasibility. To satisfy diverse performance requirements, identifying an optimal configuration of mix parameters is essential. Consequently, multi-objective optimization techniques have gained prominence in material research. Common methods include genetic algorithms (GA), particle swarm optimization (PSO), ant colony optimization (ACO), grey relational analysis (GRA), and Desirability Function Analysis (DFA). Among these, DFA offers a practical approach by allowing the simultaneous optimization of multiple responses within a bounded desirability framework.

In this study, DFA was employed to optimize the key performance indicators (compressive strength, split tensile strength, flexural strength, and cost) of AAC mixes incorporating varying FA/GGBFS ratios and NaOH molarities. The cost analysis was focused exclusively on the alkaline activator components, specifically sodium hydroxide (NaOH) and sodium silicate (Na_2SiO_3), due to their disproportionately high-cost contribution to AAC production. The economic impact of different molarity levels was assessed based on the dosage of these activators per cubic metre of concrete, as detailed in Table 3.

However, this focused cost analysis did not capture the full economic footprint of AAC production. Key inputs, such as the costs of aggregates, fly ash, GGBFS, water, admixtures, labour, transportation, energy and equipment were not included. These parameters vary based on regional availability, production scale, and procurement strategies and their exclusion limits the comprehensiveness of the current analysis.

To overcome this limitation, future work will adopt a Life Cycle Cost Analysis (LCCA) approach. This will incorporate both the direct and indirect costs associated with material sourcing, manufacturing, placement and long-term durability. Additionally, LCCA considers environmental externalities, including carbon emissions and potential tax incentives thus enabling a holistic assessment of AAC's technical and economic sustainability for real-world applications.

5.7. Desirability Function Analysis (DFA)

The DFA was first proposed by Harrington [31] and became well-known after the publication of article by Derringer et al. [32]. Researchers have applied DFA to several machining processes, including EDM, for multi-response optimization [33]. In the DFA approach, a process is deemed unacceptable if any response falls outside specified limits. The goal was to identify a set of optimal mixing configurations that produce the highest

possible individual response values. After converting each quality indicator to fit within the range of [0, 1], the individual desirability index was determined. The composite desirability index was then calculated using the weighted geometric mean of each pair of response variables. The most desirable quality attributes under examination are produced by data sets with the highest composite desirability, regarded as the optimal parameter settings.

5.8. Implementation of DFA

The highest mechanical performance was achieved for the mix with a 50% FA–50% GGBFS ratio at 16M NaOH, yielding a compressive strength of 71.4 MPa, flexural strength of 11.3 MPa, and split tensile strength of 3.84 MPa. In contrast, the lowest material cost was recorded for the mix with 8M NaOH and 100% FA, due to the lower activator content and absence of GGBFS. These findings reveal a trade-off between strength and cost, as mixes optimized for one parameter often compromise the other.

To address this conflict, Desirability Function Analysis (DFA) was employed to optimize all key responses simultaneously. A desirability threshold of di ≥ 0.1 was applied to prevent the exclusion of valid mixes influenced by cost extremes. Additionally, the environmental impact of key materials was incorporated using CO_2 emission factors sourced from literature: 1.5 kg CO_2/kg NaOH [34] and 0.07 kg CO_2/kg GGBFS [35]. These were integrated into a composite cost-sustainability factor, combining both economic and environmental objectives.

To ensure balanced optimization, equal weights (w = 0.167) were assigned to each of the six response variables: compressive strength (CS), split tensile strength (ST), flexural strength (FT), cylindrical compressive strength (CCS), cost, and CO_2 emissions. This equal weighting approach was adopted to reflect the multi-objective nature of optimization, where no single criterion is inherently more important than the others. It also aligns with sustainable engineering practices that value environmental and economic performance equally alongside structural integrity.

Balanced Importance: All performance indicators, including mechanical strengths and cost, are critical in evaluating the practical viability of alkali-activated concrete. Assigning equal weights ensures that none of the parameters disproportionately influences the optimization outcome.

Consistency with Prior Studies: Previous works (e.g., [33]) utilizing DFA in concrete and material optimization contexts have adopted equal weighting schemes, especially in the absence of clearly dominant or application-specific criteria.

Generalized Framework: Equal weights offer a neutral baseline, allowing the optimization to remain broadly applicable across different use cases (e.g., structural vs. non-structural applications), without bias toward strength or economy alone. For application-specific scenarios, this framework can be adapted by assigning custom weights based on stakeholder priorities or project-specific performance criteria.

To standardize and evaluate each desirability index within the [0 1] range, a larger-the-better desirability function is applied for strengths, while a smaller-the-better desirability function is used for costs. When the goal is to maximize the response, the desirability function outlined in Eq. 1 is employed to characterize the larger-the-better type of quality attribute. Here, y_{min} and y_{max} are the lower and upper values of the response y_i.

$$d_i = \begin{cases} 1 \\ 0 \\ \left(\frac{y_i - y_{min}}{y_{max} - y_{min}}\right)^s \end{cases}, \begin{matrix} y_i < y_{min} \\ y_{min} \le y_{tar} \le y_{max}, s \ge 0 \\ y_i > y_{max} \end{matrix} \quad (1)$$

When y_i exceeds y_{max}, individual desirability (d_i), the most desired state, becomes 1.

When y_i is less than y_{min}, individual desirability is reduced to "0", indicating an undesirable state, while di values remain within the [0 1] range for all other cases. For responses that need to be minimized, the smaller-the-better-quality characteristic, as defined by Eq. 2, is applied.

$$d_i = \begin{cases} 1 \\ 0 \\ \left(\frac{y_i - y_{max}}{y_{min} - y_{max}}\right)^s \end{cases}, \begin{matrix} y_i < y_{min} \\ y_{min} \le y_{tar} \le y_{max}, s \ge 0 \\ y_i > y_{max} \end{matrix} \quad (2)$$

The optimal scenario in this context arises when y_i is less than y_{min}, leading to an individual desirability index of 1. As y_i diverges from y_{min}, the d_i value diminishes until it becomes "0" when y_i surpasses y_{max}. In all other cases, di values fall within the range of [0 1]. The geometric mean of the individual desirability is used to calculate the composite desirability for each of the experimental conditions, and the result is given by Eq. 3. The weights given to various responses according to their relative relevance make up the exponent r.

$$CD = (d_1^{w1} \times d_2^{w2} \times d_3^{w3} \times ..)^{\frac{1}{k}} \quad (3)$$

where k denotes the number of variables and d_1, d_2, and d_3 denote the various desirability indices The weighted responses are w1, w2, and w3 such that $w = \sum_i^k w_i = 1$. If any of the responses are undesirable, the CD is equal to zero or $d_i = 0$. Using the desirability functions offered by Eqs. 1 and 2, we can determine an individual's desirability of strengths and cost. The weights (w_1=w_2=w_3=w_4=w_5=w_6=0.167) for strengths, cost and CO_2 are equal. Eq. 3 is used to determine CD while considering the six responses under study. Table 5 shows the highest CD recorded as 0.9451. The corresponding individual desirability indices are 0.9359 for maximum compressive strength, 0.9354 for flexural strength, and 0.8662 for split tensile strength, cylindrical compressive strength (0.9951) and minimum CO_2 emissions (0.9446) cost is (1.0) is obtained for 50% FA/GGBFS and molarity ratio at 8M.

Table 5. Estimated desirability values incorporating strength, cost, and CO_2 emissions for multi-objective optimization using DFA

StdOrder	MOL	FA/GGBFS	CS (MPa)	ST (MPa)	FS (MPa)	CCS (MPa)	Cost (US $/m^3)	CO_2 Emissions (kg/m^3)	CS-max	ST-max	FT-max	CCS-max	Cost (min)	CO2-min	Composite Desirability	Rank
1	8	25	36.95	2.9	7.5	18.32	84.86	58.11	0.7190	0.0000	0.6516	0.3907	1.0000	0.9095	0.0000	7
2	**8**	**50**	**58.3**	**3.51**	**9.3**	**21.01**	**84.86**	**49.71**	**0.9359**	**0.9354**	**0.8662**	**0.9951**	**1.0000**	**0.9446**	**0.9451**	**1**
3	8	75	47.8	3.21	7.4	19.43	84.86	41.31	0.8617	0.8354	0.6210	0.8591	1.0000	0.9743	0.8489	5
4	8	100	31.4	3.01	7.1	18.31	84.86	32.91	0.0000	0.7027	0.0000	0.0000	1.0000	1.0000	0.0000	7
5	12	25	61.1	3.4	8.9	19.98	93.72	74.57	0.9515	0.9048	0.8376	0.9184	0.8907	0.8101	0.8842	4
6	**12**	**50**	**66.3**	**3.71**	**9.9**	**21.09**	**93.72**	**66.17**	**0.9775**	**0.9807**	**0.9018**	**1.0000**	**0.8907**	**0.8678**	**0.9350**	**2**
7	12	75	57.75	3.5	9.4	21.09	93.72	57.77	0.9327	0.9328	0.8726	1.0000	0.8907	0.9110	0.9224	3
8	12	100	41.4	3.49	7.3	18.87	93.72	49.37	0.7933	0.9302	0.5804	0.7652	0.8907	0.9459	0.8070	6
9	16	25	58.3	3.5	8.2	21.09	102.59	91.04	0.9359	0.9328	0.7715	1.0000	0.0000	0.0000	0.0000	7
10	16	50	71.4	3.81	12.3	19.98	102.59	82.64	1.0000	1.0000	1.0000	0.9184	0.0000	0.7239	0.0000	7
11	16	75	69.85	3.61	9.8	19.98	102.59	74.24	0.9934	0.9594	0.8963	0.9184	0.0000	0.8128	0.0000	7
12	16	100	48.1	3.59	8.1	19.11	102.59	65.83	0.8643	0.9548	0.7593	0.8122	0.0000	0.8698	0.0000	7

5.9. Comparative Assessment of 8M and 12M FA–GGBFS AAC Mixes Using DFA

Desirability Function Analysis (DFA) provides a thorough assessment of alkali-activated concrete (AAC) mixes by optimizing six parameters simultaneously: compressive strength, split tensile strength, flexural strength, cylindrical compressive strength, cost, and CO_2 emissions. Incorporating the environmental impact through embodied CO_2 emissions offers a realistic perspective for evaluating mix viability in terms of both structural integrity and sustainability.

The mix with 8M NaOH and a 50% FA-50% GGBFS ratio achieved the highest composite desirability score in the CO_2 integrated DFA, making it the most optimal mix overall when structural performance, cost, and environmental impact are considered equally. This mix achieved a compressive strength of 58.3 MPa, split tensile strength of 3.51 MPa, and flexural strength of 9.3 MPa, all exceeding the minimum thresholds for general structural applications. Its performance is attributed to the synergistic activation of calcium-rich GGBFS with fly ash, even at a relatively low NaOH molarity of 8M. In terms of sustainability, the mix excelled with a moderate CO_2 emission level of 49.71 kg/m^3 and the lowest cost among the high-strength mixes (US \$84.86/m^3). The lower molarity not only reduces the environmental burden of NaOH production (1.5 kg CO_2/kg) but also enhances economic feasibility. Low molarity significantly reduces embodied carbon while maintaining mechanical performance, making it the most eco-efficient and cost-effective mix in this study [36]. By consistently scoring high across all six DFA metrics, this mix presents an ideal solution for eco-efficient structural concrete. It offers a superior balance between strength and sustainability without requiring high activator concentrations or specialized curing. As such, it is well suited for structural applications in moderate-load environments, such as slabs, footings, and precast members.

In contrast, the 12M 50% FA-50% GGBFS mix delivered the highest overall mechanical performance among all sustainable options, with a compressive strength of 66.3 MPa, split tensile strength of 3.71 MPa and flexural strength of 9.9 MPa. While its cost (US \$93.72/m^3) and CO_2 emissions (66.17 kg/m^3) were moderately higher than those of its 8M counterpart, it ranked second overall due to its superior structural characteristics. This makes it highly suitable for load-bearing applications where the mechanical properties cannot be compromised.

The 16M mixes, despite showing the highest strength values, were penalized due to their high activator costs and elevated CO_2 footprints, indicating a diminishing return at higher molarities.

Together, these two mixes demonstrate the effectiveness of multi-objective optimization. The 8M mix is ideal for eco-efficient, low-carbon construction, while the 12M mix offers a strong balance between structural performance and sustainability, both of which are excellent mixtures for large-scale adoption in AAC-based infrastructure. The method also highlights the importance of context-specific optimization mixes ideal for structural loads may differ from those chosen for low-impact or mass applications.

6. Conclusions

The workability and the mechanical properties of alkali activated concrete using fly ash and GGBFS were investigated at ambient cured temperature. Based on the investigations carried out in the present study, the following conclusions are drawn:

- Alkali-activated concrete (AAC) can be produced in a similar manner to conventional Portland cement concrete using ambient curing. The use of a low-molarity alkaline solution enabled effective geopolymerization without the need for elevated temperatures, making AAC suitable for field applications in tropical climates.
- The mechanical properties, including the compressive strength, flexural strength, and split tensile strength, improved with increasing NaOH molarity from 8M to 16M. However, higher molarity also led to reduced workability.
- Workability, measured by slump, decreased by approximately 50% when the NaOH molarity was increased from 8M to 16M, particularly in GGBFS rich mixes. This was attributed to the high viscosity and short setting time of the concentrated alkaline solutions.
- The setting time was observed to decrease with increasing GGBFS content, indicating its potential to accelerate early age strength gain in AAC systems.
- Optimal mechanical performance was achieved with a 50:50 FA-GGBFS blend, delivering the highest compressive strength (71.4 MPa), split tensile strength (3.84 MPa), and flexural strength (12.3 MPa) at 16M NaOH.
- Based on multi-objective optimization using Desirability Function Analysis (DFA) with equally weighted criteria (strengths, cost, CO_2), the most balanced mix was obtained with 12M NaOH with 50% FA–50% GGBFS, offering excellent strength and moderate sustainability.
- The top-ranked mix in terms of composite desirability was the 8M–50% FA-GGBFS combination, which provided sufficient strength, the lowest cost, and low CO_2 emissions (49.71 kg/m^3), making it highly suitable for sustainable construction with moderate structural demands.
- The low standard deviations within ±5–8% of the mean observed in compressive, split tensile and flexural strength results confirm the repeatability and reliability of the optimized AAC mixes under ambient curing conditions.

- Future work should focus on the life cycle cost and carbon accounting of AAC production and explore the use of renewable-based activators. Additionally, ambient curing combined with GGBFS inclusion offers a practical pathway for eliminating the environmental burden of oven curing in geopolymer concrete production.

Acknowledgements

The authors express sincere thanks to the Management and Principal of Vasavi College of Engineering (A), Hyderabad, for supporting the experimental work in the college laboratories. The help of Undergraduate students during laboratory experimentation is also acknowledged.

Conflict of Interest Declaration

The authors declare that they have no affiliations with or involvement in any organization or entity with any financial interest in the subject matter or materials discussed in this manuscript.

REFERENCES

[1] V. M. Malhotra and A. Bildeau, "High volume flyash system: The concrete solutions for sustainable Development," in Proc of International Symposium on concrete Technology for Sustainable Development in the twenty first century, Hyderabad, India, February 9-11 1999, pp. 43-54,

[2] M. C. G. Juenger, F. Winnefeld, J. L. Provis, and J. H. Ideker, "Advances in alternative cementitious binders," Cement and Concrete Research, vol. 41, no. 12, pp. 1232-1243, 2011. https://doi.org/10.1016/j.cemconres.2010.11.012

[3] S. Kumar, R. Kumar, A. Bandopadhyay, T. C. Alex, B. Ravi Kumar, S. K. Das, and S. P. Mehrotra, "Mechanical activation of granulated blast furnace slag and its effect on the properties and structure of portland slag cement," Cement and Concrete Composites, vol. 30, no. 8, pp. 679-685, 2008. https://doi.org/10.1016/j.cemconcomp.2008.05.005.

[4] S. Kumar, R. Kumar, and S. P. Mehrotra, "Influence of granulated blast furnace slag on the reaction, structure and properties of fly ash based geopolymer," Journal of Materials Science, vol. 45, no. 3, pp. 607-615, 2010. https://doi.org/10.1007/s10853-009-3934-5.

[5] S. A. Bernal, J. Bejarano, C. Garzón, R. Mejía de Gutiérrez, S. Delvasto, and E. D. Rodríguez, "Performance of refractory aluminosilicate particle/fiber-reinforced geopolymer composites," Composites Part B: Engineering, vol. 43, no. 4, pp. 1919-1928, 2012. https://doi.org/10.1016/j.compositesb.2012.02.027.

[6] J. Davidovits, "Geopolymer properties and chemistry," in 1st European conference on soft minerallurgy, geopolymer 88 Compiegne, France, 1998: Geopolymer Institute,

[7] N. P. Rajamane, "Studies on development of ambient temperature cured fly ash and GGBS based geopolymer concretes," Phd thesis submitted to Visvesvaraya Technological University, Belgaum, Karnataka, 2013.

[8] N. T. Sithole and T. Mashifana, "Geosynthesis of building and construction materials through alkaline activation of granulated blast furnace slag," Construction and Building Materials, vol. 264, p. 120712, 2020. https://doi.org/10.1016/j.conbuildmat.2020.120712.

[9] A. S. Albidah, "Effect of partial replacement of geopolymer binder materials on the fresh and mechanical properties: A review," Ceramics International, vol. 47, no. 11, pp. 14923-14943, 2021. https://doi.org/10.1016/j.ceramint.2021.02.127.

[10] Y. Jeong, H. Park, Y. Jun, J. H. Jeong, and J. E. Oh, "Influence of slag characteristics on strength development and reaction products in a CaO-activated slag system," Cement and Concrete Composites, vol. 72, pp. 155-167, 2016. https://doi.org/10.1016/j.cemconcomp.2016.06.005.

[11] P. Pavithra, M. Srinivasula Reddy, P. Dinakar, B. Hanumantha Rao, B. K. Satpathy, and A. N. Mohanty, "Effect of the Na_2SiO_3/NaOH Ratio and NaOH Molarity on the Synthesis of Fly Ash-Based Geopolymer Mortar," Proceedings/Geo-Chicago 2016, pp. 336-344, 2016. https://doi.org/10.1061/9780784480151.034.

[12] S. Puligilla and P. Mondal, "Role of slag in microstructural development and hardening of fly ash-slag geopolymer," Cement and Concrete Research, vol. 43, pp. 70-80, 2013. https://doi.org/10.1016/j.cemconres.2012.10.004

[13] S. S. Pradhan, U. Mishra, S. K. Biswal, and P. Jangra, "Development of sustainable slag-based alkali-activated concrete incorporating fly ash at ambient curing conditions," Energy, Ecology and Environment, vol. 9, no. 5, pp. 563-577, 2024. https://doi.org/10.1007/s40974-024-00319-7.

[14] A. Y. Osman and M. R. and Irshidat, "Comprehensive evaluation of microstructure and mechanical performance of sustainable ambient-cured alkali-activated composites," Journal of Sustainable Cement-Based Materials, vol. 13, no. 10, pp. 1552-1566, 2024. https://doi.org/10.1080/21650373.2024.2399650

[15] M. Maheswaran, C. F. Christy, M. Muthukannan, K. Arunkumar, and A. Vigneshkumar, "Parametric study on the performance of industrial byproducts based geopolymer concrete blended with rice husk ash & nano silica," Research on Engineering structures & Materials, vol. 9, no. 4, pp. 1267–1285, 2023. https://doi.org/10.17515/resm2023.809ma0703.

[16] R. R. Samuvel, G. P. Arulraj, N. Anand, B. Kanagaraj, and E. Lubloy, "Eco-friendly alkali-activated nano concrete: Impact of nano-GGBFS on mechanical and microstructural properties," Case Studies in Chemical and Environmental Engineering, vol. 11, p. 101131, 2025. https://doi.org/10.1016/j.cscee.2025.101131.

[17] N. P. Tran, T. N. Nguyen, J. R. Black, and T. D. Ngo, "High-temperature stability of ambient-cured one-part alkali-activated materials incorporating graphene

nanoplatelets for thermal energy storage," Developments in the Built Environment, vol. 18, p. 100447, 2024. https://doi.org/10.1016/j.dibe.2024.100447.

[18] B.R. Arun, J.M. Srishaila, S. Md. Khalid, A. Veerabhadrappa, K. Kavyashree, and H. M. Tanu, "Prediction of machine learning application in the development of novel sustainable self-compacting geopolymer concrete," Research on Engineering structures & Materials, vol. 11, no. 4, pp. 1469-1490, 2025. https://doi.org/10.17515/resm2024.354ma0716rs.

[19] A. Esparham, A. B. Moradikhou, F. K. Andalib, and M. J. Avanaki, "Strength characteristics of granulated ground blast furnace slag-based geopolymer concrete," Advances in concrete construction, vol. 11, no. 3, pp. 219-229, 2021. https://doi.org/10.12989/acc.2021.11.3.219.

[20] B. B. Jindal, "Feasibility study of ambient cured geopolymer concrete–A review," Advances in concrete construction, vol. 6, no. 4, pp. 387-405, 2018. https://doi.org/10.12989/acc.2018.6.4.387.

[21] S. Paruthi, I. Rahman, A. H. Khan, N. Sharma, and A. Alyaseen, "Strength, durability, and economic analysis of GGBS-based geopolymer concrete with silica fume under harsh conditions," Scientific Reports, vol. 14, no. 1, p. 31572, 2024. https://doi.org/10.1038/s41598-024-77801-z.

[22] S. Ament, A. Witte, N. Garg, and J. Kusuma, "Sustainable concrete via Bayesian optimization," arXiv preprint arXiv:2310.18288, 2023. https://doi.org/10.48550/arXiv.2310.18288.

[23] D. Hardjito and B. V. Rangan, "Development and properties of low-calcium fly ash-based geopolymer concrete," Research report GC 1, Curtin University of technology Perth, Australia., 2005.

[24] IS:516-2021 "Part 1: Sec 1: Hardened concrete Section 1 compressive, flexural and split tensile strength (First Revision)," Bureau of Indian Standards, New Delhi, India.

[25] B. Sun, Y. Sun, G. Ye, and G. De Schutter, "A mix design methodology of slag and fly ash-based alkali-activated paste," Cement and Concrete Composites, vol. 126, p. 104368, 2022. https://doi.org/10.1016/j.cemconcomp.2021.104368.

[26] M. F. A. Abdul Sani, R. Muhamad, and K. H. Mo, "Effect of Ground Granulated Blast Furnace Slag as Partial Replacement in Fly Ash-Based Geopolymer Concrete," IOP Conference Series: Materials Science and Engineering, vol. 712, no. 1, p. 012002, 2020. https://doi.org/10.1088/1757-899X/712/1/012002.

[27] S. Banchhor, M. Murmu, and S. V. Deo, "Combined effect of fly-ash and GGBS on performance of alkali activated concrete," Journal of Building Pathology and Rehabilitation, vol. 7, no. 1, p. 32, 2022. https://doi.org/10.1007/s41024-022-00170-5.

[28] B. Pratap, R. K. Paswan, and P. Kumar, "Mechanical and micro-characterization of alkali-activated concrete under high-temperature exposure," Structural Concrete, vol. 26, no. 2, pp. 1911-1923, 2025. https://doi.org/10.1002/suco.202301157.

[29] X. Wang, F. Liu, L. Li, W. Chen, X. Cong, T. Yu, and B. Zhang, "Study on the Compressive Strength and Reaction Mechanism of Alkali-Activated Geopolymer Materials Using Coal Gangue and Ground Granulated Blast Furnace Slag," Materials, vol. 17, no. 15, p. 36592024, 2024. https://doi.org/10.3390/ma17153659.

[30] R. M. Waqas, F. Butt, X. Zhu, T. Jiang, and R. F. Tufail, "A Comprehensive Study on the Factors Affecting the Workability and Mechanical Properties of Ambient Cured Fly Ash and Slag Based Geopolymer Concrete," Applied Sciences, vol. 11, no. 18, p. 87222021, https://doi.org/10.3390/app11188722.

[31] E. C. Harrington, "The desirability function," Industrial quality control, vol. 21, no. 10, pp. 494-498, 1965.

[32] G. Derringer and R. Suich, "Simultaneous Optimization of Several Response Variables," Journal of Quality Technology, vol. 12, no. 4, pp. 214-219, 1980. https://doi.org/10.1080/00224065.1980.11980968.

[33] Z. Zhang, J. L. Provis, A. Reid, and H. Wang, "Fly ash-based geopolymers: The relationship between composition, pore structure and efflorescence," Cement and Concrete Research, vol. 64, pp. 30-41, 2014. https://doi.org/10.1016/j.cemconres.2014.06.004

[34] E. Medina-Martos, J.-L. Gâvez-Martos, J. Almarza, C. Lirio, D. Iribarren, A. Valente, and J. Dufour, "Environmental and economic performance of carbon capture with sodium hydroxide," Journal of CO2 Utilization, vol. 60, p. 101991, 2022. https://doi.org/10.1016/j.jcou.2022.101991.

[35] D. Munro, G. Di Benedetto, M. Graham, M. Jans-Singh, M. Turpin, and F. Kanavaris, "The assessment of the embodied carbon of resource-constrained materials including ground granulated blast-furnace slag (GGBS) and ferrous scrap," Structures, vol. 78, p. 109175, 2025. https://doi.org/10.1016/j.istruc.2025.109175.

[36] S. Karthik and K. S. Mohan, "A Taguchi Approach for Optimizing Design Mixture of Geopolymer Concrete Incorporating Fly Ash, Ground Granulated Blast Furnace Slag and Silica Fume," Crystals, vol. 11, no. 11, 2021, https://doi.org/10.3390/cryst11111279.